BLOOD VESSELS EXTRACTION USING FUZZY MATHEMATICAL MORPHOLOGY

Daniel Oliveira Dantas, Diego de Souza Oliveira, Helton Danilo Passos Leal

Universidade Federal de Sergipe
Departamento de Computação

ABSTRACT

Blood vessel extraction from retinography images is useful for detection of many retinopathies. In this paper we propose a way to improve blood vessel detection by use of Fuzzy Mathematical Morphology (FMM) operators. The proposed pipeline, although simple, was found to have the highest accuracy on the STARE dataset, and second highest on the DRIVE dataset. We also present a parallel implementation of the FMM operators, in OpenCL, up to about 500 times faster than their counterpart in C++.

Index Terms— Fuzzy Mathematical Morphology, Retinography, OpenCL, Segmentation

1. INTRODUCTION

Blood vessel extraction from retinography images is useful for detection of many retinopathies. Among the retinopathies are glaucoma, arteriosclerosis [1], diabetic retinopaty (DR) and age-related macular degeneration (AMD) [2].

A few works do not rely on lesion and vessel segmentation, as the work by Agurto [2]. These are known as top-down approaches. On the other hand, bottom-up approaches, based on lesion and vessel detection, are much more common.

Many methods have been proposed to detect blood vessels in the retina. In the literature, the best results we could find use approaches based on matched filters to detect the vessels [3, 4, 5, 6, 7], based on centerlines [8, 9, 10], curvelet transforms [11, 7], supervised learning [12, 13, 14, 15], graph-cut [16] and region growing [17].

In this paper we propose a way to improve blood vessel detection by use of Fuzzy Mathematical Morphology (FMM) operators. The proposed method is very simple, and does not require training as the supervised methods, nor different types of masks, as the matched filter approaches. In spite of simplicity, is among the most accurates in literature. We also present a parallel implementation of the FMM operators, in OpenCL, much faster than their conterpart, in C++.

The FMM operators were implemented as a module of the library VisionGL [18, 19]. VisionGL is an open source library that helps creating image processing operators and systems by generating automatically wrapper code and optimizing image transfers between RAM and GPU.

2. BACKGROUND

To understand the proposed algorithm, a brief description of the used operations is given in this section.

2.1. Mathematical Morphology

Mathematical Morphology (MM) is a theoretical framework widely used in image processing problems. Provides a broad range of tools used in microscopy, document procesing, inspection, pattern recognition, robot vision among other areas. Is based on probing images by small geometric patterns called *structuring elements*. The most basic operations in MM are the erosion and its dual, the dilation [20].

Mathematical morphology was first described in binary images and later generalized to gray-scale images. An erosion by a flat structuring element is defined by

$$(f \ominus S)(x) = \min\{f(x+z) : z \in S\} \tag{1}$$

where f is a gray-scale input image, S is a set of pixel coordinates centered at origin, x are the coordinates of a pixel in the input image, and z are the coordinates of a pixel in S. This definition can be applied to binary images if they are considered a particular type of gray-scale images with pixel values in the set $\{0, 1\}$. Similarly, the dilation of f by S is defined by

$$(f \oplus S)(x) = \max\{f(x-z) : z \in S\} \tag{2}$$

A useful operator, defined as a composition of a dilation and an erosion, is the closing. Closing is used to close small holes and narrow valleys, and is defined by

$$f \bullet S = (f \oplus S) \ominus S \tag{3}$$

Other useful operations is the closing top-hat (black-hat). Black-hat leaves only the narrow valleys of the input image, and is defined by

$$f \,\hat{\bullet}\, S = (f \bullet S) - f \tag{4}$$

To understand the reconstruction operations, we must define the operation of conditional dilation. A dilation of f by S conditioned by g is given by

$$f \oplus_g S = (f \oplus S) \wedge g \tag{5}$$

where $\wedge$ denotes the pixewise minimum of two images.

The reconstruction operations known as opening by reconstruction consists on eroding the input image f and then dilating the result conditioned by f until stabilization, i.e., the output of a dilation is the same of its input. Can be formalized as

$$f \,\tilde{\circ}\, S = ((f \ominus S) \oplus_f S)^{\infty} \quad (6)$$

These operations can be generalized to Fuzzy Mathematical Morphology, which will be defined in the next subsection, by replacing the dilation and erosion operations.

2.2. Fuzzy Mathematical Morphology

Fuzzy Mathematical Morphology (FMM) is a generalization of MM that combines it with fuzzy logic. Usually FMM image processing gives better results in noisy images [21]. The basic operations of erosion and dilation are defined in a different way. Fuzzy dilations are defined by

$$(f \oplus^F S)(x) = \max_{z \in S}\{C(f(x+z), S(z))\} \quad (7)$$

where C is a conjuntion operation. Similarly, fuzzy erosions are defined by

$$(f \ominus^F S)(x) = \min_{z \in S}\{D(f(x+z), 1 - S(z))\} \quad (8)$$

where D is a disjunction operation. Please notice that the input image is normalized, by a linear transformation, to the dynamic interval $[0, 1]$. A grayscale value with eight bits, for example, with dynamic range in $\{0, 1, ..., 255\}$, would be normalized by dividing it by 255. Structuring elements, instead of a set of pixels as seen in Subsection 2.1, are a small image. Table 1 shows eight types of FMM and respective conjunctions and disjunctions. More details about FMM and its properties are thoroughly discussed by Bouchet et al [22, 21].

3. METHOD

In this work was developed a pipeline for segmenting blood vessels in retinal images with FMM operations. The general steps of the pipeline are: green channel extraction, mask creation, Gaussian blur, black-hat, thresholding and opening by reconstruction.

The first step, green channel extraction, is very common when dealing with retinography images. In red and blue channels, the vessels are not as evident as in green channel, so, these two channels are discarded, and only the green channel is used in the process. An example of the three channels after separation is shown in Figures 1(a), 1(b) and 1(c).

It is important to create a mask that separates the region of interest from the external part of the image, which should be ignored. The mask is created, as soon as the green channel is obtained, by a simple threshold with constant parameter equal to the grayscale 20. Figure 1(d) shows a mask example.

Afterwards, a Gaussian blur is applied to the image to reduce noise. The Gaussian window is a square window containing an isotropic Gaussian function. This step has two parameters: window size and Gaussian standard deviation. Figure 1(e) shows an example of blur applied to the input image green channel.

The step after the blur is the black-hat. As can be seen in Figure 1(e), the blood vessels are darker than the surrounding region. To segment the blood vessels, a black-hat is used, as described in Equation 4. In the pipeline, the black-hat operation has three parameters: the FMM method, structuring element size, and number of dilations and erosions. Figure 1(f) shows an example of black-hat result.

At this point, the mask, obtained in the beginning of the process, is applied. By applying the mask we mean that the minimum between the current result and the mask is obtained.

After that, a threshold is applied. A few different threshold values were tested. After the threshold, the result can be quite noisy, having peaks not connected to the blood vessels. Figure 1(g) shows an example of threshold result and it's noise.

To solve this problem, an opening by reconstruction is done. The opening by reconstruction is defined by Equation 6 The effect of this operation is to eliminate the disconnected small peaks, and only the small details connected to the main vessels remain in the end of the process. The parameters of this step are two: the FMM method, and the strucuring element size, both are the same as in the black-hat step. At this point, another threshold is applied, with constant parameter equal to the grayscale 1. Figure 1(h) shows the final result after reconstruction with a fuzzy standard opening by reconstruction.

4. RESULTS

To create our pipeline, we implemented FMM operators in OpenCL in order to run them in the GPU. We compared the processing times of operators implemented in OpenCL and C++ running in the GPU and CPU respectively. Results are shown in Table 2. Speedups between 210 and 518 times, in Hamacher and Geometric fuzzy dilation respectively, were obtained. The benchmarks were obtained in a Core I7 computer with GPU Radeon R9 270x.

To asses the accuracy or the proposed pipeline, we tested it with 40 images from the dataset DRIVE [23, 13], and 20 images from the dataset STARE [24]. Accuracy measures were obtained by comparing our segmentation with the groundtruth provided by the first specialist in DRIVE, and by Hoover in STARE dataset.

As explained in Section 3, the pipeline is parameterized. The parameters are six: method (id), structuring element size (seSize), number of dilations and erosions in black-hat (nBh),

ID	Name	Conjunction	Disjunction
1	Standard	$C(a,b)=\min(a,b)$	$D(a,b)=\max(a,b)$
2	Algebraic	$C(a,b)=ab$	$D(a,b)=a+b-ab$
3	Bounded	$C(a,b)=\max(0,a+b-1)$	$D(a,b)=\min(1,a+b)$
4	Drastic	$C(a,b)=\begin{cases} a & \text{if } b=1 \\ b & \text{if } a=1 \\ 0 & \text{otherwise} \end{cases}$	$D(a,b)=\begin{cases} a & \text{if } b=0 \\ b & \text{if } a=0 \\ 1 & \text{otherwise} \end{cases}$
5	Dubois & Prade	$C(a,b)=\frac{ab}{\max(a,b,\gamma)}$	$D(a,b)=1-\frac{(1-a)(1-b)}{\max(1-a,1-b,1-\gamma)}$
6	Hamacher	$C(a,b)=\frac{ab}{\gamma+(1-\gamma)(a+b-ab)}$	$D(a,b)=1-\frac{a+b-(\gamma-2)ab}{1+(\gamma-1)ab}$
7	Geometric	$C(a,b)=[ab]^{\frac{1}{2}}$	$D(a,b)=1-[(1-a)(1-b)]^{\frac{1}{2}}$
8	Arithmetic	$C(a,b)=\left[\frac{\min(a,b)(a+b)}{2}\right]^{\frac{1}{2}}$	$D(a,b)=1-\left[\frac{\min(1-a,1-b)(2-a-b)}{2}\right]^{\frac{1}{2}}$

Table 1. Conjunctions and disjunctions

Gaussian blur window size (wSize), Gaussian blur standard deviation (wSd), and threshold (th). The γ used was 0.2.

The method (id) parameter selects what kind of morphological operation is used. Varies from 1 to 9, where 1 to 8 are the fuzzy methods listed in Table 1. The method 9 refers to the classic MM operators, i.e., non-fuzzy. Actually, the methods 4, 7 and 8 don't give useful results, so, we will list only the results of six methods. Morphological operations are used in the black-hat and reconstruction steps.

The structuring element size (seSize) parameter indicates the side in pixels of a square structuring element. It is used in the black-hat and reconstruction steps. The tested values were 3, 5, 7 and 9. The fuzzy structuring element is an isotropic Gaussian with $\sigma = r/5$, where the radius $r = (\text{seSize-}1)/2$. The classic structuring element is a flat box.

The number of dilations and erosions in black-hat (nBh) specifies how many times the dilation and erosion are repeated in the black-hat step. The effect is the same as using a bigger structuring element, but is much faster. The tested values were 1 and 2.

The Gaussian blur window size (wSize) parameter specifies the side of the square Gaussian blur mask. The tested values were 3, 5, 7 and 9. The Gaussian blur standard deviation (wSd) specifies the standard deviation of the Gaussian function. The tested values were 1, 2, 3 and 4.

Finally the threshold (th) parameter specify the grayscale values of the threshold operation done just before the reconstruction. The tested values were 3, 4 and 5.

The tested values were selected empirically, after some tests, in order to maximize the probability to obtain useful results. Values that often gave bad results were ruled out. All the possible combinations of selected values were tested.

The best results obtained with the dataset DRIVE are listed and compared with results from other works in Table 3. Results obtained with the dataset STARE are listed in Table 4. In both tables are shown the true positive rate (TPR), false positive rate (FPR) and accuracy (ACC) of each method.

ID	Name	GPU	CPU
1	Standard	0.25	126
2	Algebraic	0.25	102
3	Bounded	0.31	137
4	Drastic	0.26	113
5	Dubois & Prade	0.54	163
6	Hamacher	0.55	116
7	Geometric	0.33	171
8	Arithmetic	0.42	198

Table 2. Processing times of a fuzzy dilation, by a 3x3 structuring element, in milliseconds, on a grayscale image with 565x584 pixels

As seen in Table 3, the accuracy of the proposed methods are better than all methods found in literature, except for one, proposed by Kar [7]. In Table 4, the proposed fuzzy methods are better than all the other results found in literature.

We can also see, from both tables, that results obtained with FMM operators are slightly better than results obtained with classic opearators, i.e., non-fuzzy.

5. CONCLUSIONS

In this work we propose a pipeline for segmentation of retina blood vessels using MM operators, both fuzzy and non-fuzzy. Although simple, the pipeline with fuzzy operators provides better results than all previous publications except one. Results also show that, by replacing classic MM operations with FMM ones, accuracy can be slightly improved.

Another contribution of this work is an open source parallel implementation of FMM operators in OpenCL, up to about 500 times faster than their counterpart in C++.

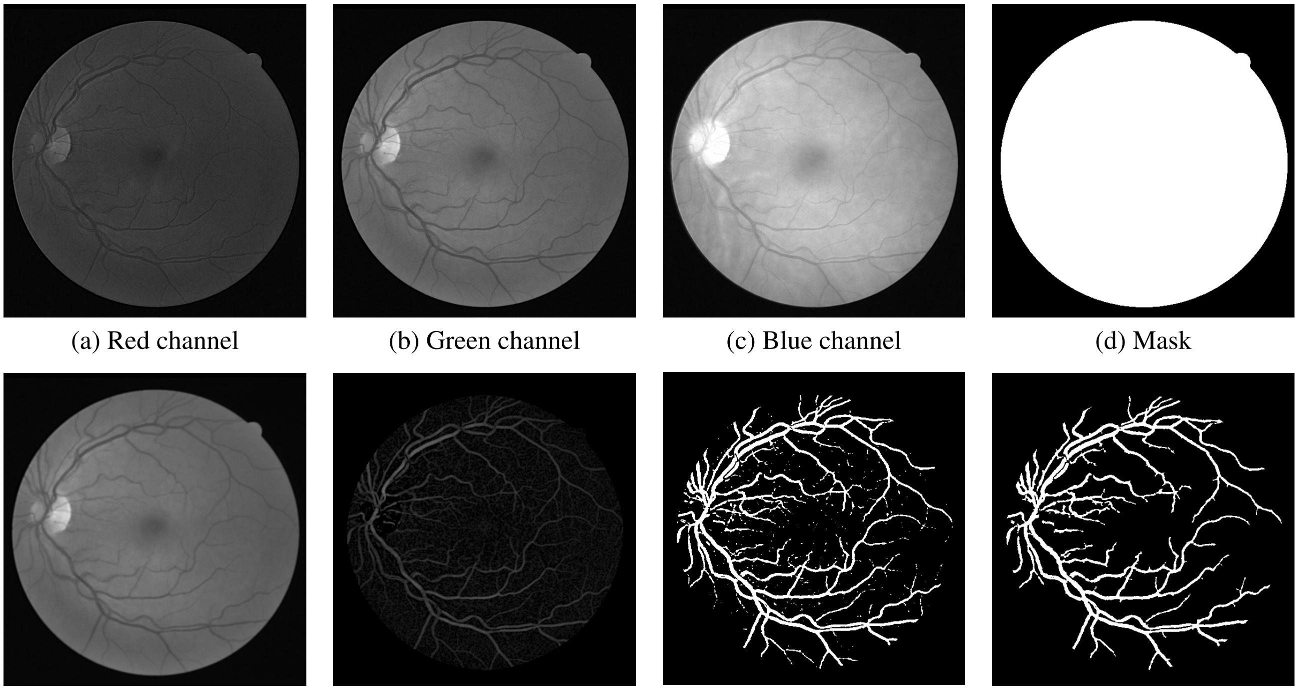

(a) Red channel (b) Green channel (c) Blue channel (d) Mask

(e) After blur (f) After black-hat (g) After threshold (h) After reconstruction

Fig. 1. Input image example and results in each step of the pipeline.

Method	Year	TPR	FPR	ACC
Chaudhuri [3]	1989	0.6168	0.0259	0.9284
Niemeijer [12]	2004	0.6898	0.0304	0.9416
Staal [13]	2004	0.7194	0.0227	0.9442
Mendona [8]	2006	0.7344	0.0236	0.9452
Soares [14]	2006	0.7285	0.0213	0.9466
Martinez-Perez [17]	2007	0.7246	0.0345	0.9344
Zhang [1]	2010	0.7120	0.0276	0.9382
Miri [11]	2011	0.7352	0.0205	0.9458
Marin [15]	2011	0.7067	0.0199	0.9452
Fraz [9]	2012	0.7152	0.0231	0.9430
Salazar-Gonzalez [16]	2014	0.7512	0.0316	0.9412
Ben-Abdallah [10]	2015	0.5879	0.0166	0.9155
Deshmukh [6]	2015	0.7120	0.0276	0.9382
Kar [7]	2015	0.7718	0.0189	0.9631
1 - Standard (5, 2, 7, 1, 5)		0.6467	0.0157	0.9550
2 - Algebraic (5, 2, 7, 1, 5)		0.6624	0.0160	0.9561
3 - Bounded (5, 2, 3, 1, 5)		0.6314	0.0128	0.9563
5 - D. & P. (5, 2, 7, 1, 5)		0.6467	0.0157	0.9550
6 - Hamacher (5, 2, 7, 1, 5)		0.6602	0.0163	0.9556
9 - Classic (3, 2, 3, 1, 3)		0.5934	0.0126	0.9531

Table 3. Comparison of vessel segmentation results on DRIVE dataset. In parenthesis are the pipeline parameters (seSize, nBh, wSize, wSd, th)

Method	Year	TPR	FPR	ACC
Chaudhuri [3]	1989	0.6134	0.0245	0.9384
Hoover [4]	2000	0.6751	0.0433	0.9267
Staal [13]	2004	0.6970	0.0190	0.9516
Mendona [8]	2006	0.6996	0.0270	0.9440
Soares [14]	2006	0.7165	0.0252	0.9480
Martinez-Perez [17]	2007	0.7506	0.0431	0.9410
Zhang [1]	2010	0.7177	0.0247	0.9484
Marin [15]	2011	0.6944	0.0181	0.9526
Fraz [9]	2012	0.7311	0.0320	0.9442
Kaba [5]	2013	0.6645	0.0216	0.9450
Salazar-Gonzalez [16]	2014	0.7887	0.0367	0.9441
Ben-Abdallah [10]	2015	0.6145	0.0162	0.9402
1 - Standard (5, 2, 7, 1, 5)		0.7163	0.0278	0.9528
2 - Algebraic (5, 2, 7, 1, 5)		0.7145	0.0255	0.9548
3 - Bounded (5, 2, 5, 2, 5)		0.5726	0.0145	0.9542
5 - D. & P. (5, 2, 7, 1, 5)		0.7163	0.0278	0.9528
6 - Hamacher (5, 2, 7, 1, 5)		0.7210	0.0273	0.9536
9 - Classic (5, 2, 7, 1, 5)		0.6901	0.0258	0.9526

Table 4. Comparison of vessel segmentation results on STARE dataset. In parenthesis are the pipeline parameters (seSize, nBh, wSize, wSd, th)

6. REFERENCES

[1] Bob Zhang et al., "Retinal vessel extraction by matched filter with first-order derivative of gaussian," *Computers in Biology and Medicine*, vol. 40, no. 4, pp. 438–445, Apr. 2010.

[2] Carla Agurto et al., "Automatic detection of diabetic retinopathy and age-related macular degeneration in digital fundus images," *Investigative Ophthalmology & Visual Science*, vol. 52, no. 8, pp. 5862–5871, July 2011.

[3] S. Chaudhuri et al., "Detection of blood vessels in retinal images using two-dimensional matched filters," *IEEE Transactions on Medical Imaging*, vol. 8, no. 3, pp. 263–269, 1989.

[4] Adam Hoover, Valentina Kouznetsova, and Michael Goldbaum, "Locating blood vessels in retinal images by piecewise threshold probing of a matched filter response," *IEEE Transactions on Medical Imaging*, vol. 19, no. 3, pp. 203–210, 2000.

[5] Djibril Kaba et al., "Segmentation of retinal blood vessels using gaussian mixture models and expectation maximisation," in *International Conference on Health Information Science*. Springer, 2013, pp. 105–112.

[6] S. J. Deshmukh and S. B. Patil, "Vessel extraction from retinal images by using matched filter and first derivative of gaussian function," *International Journal of Innovative Research in Electrical, Electronics, Instrumentation and Control Engineering*, vol. 3, no. 1, pp. 6–12, 2015.

[7] Sudeshna Sil Kar and Santi P. Maity, "Blood vessel extraction with optic disc removal in retinal images," in *Advances in Pattern Recognition (ICAPR), 2015 Eighth International Conference on*. IEEE, 2015.

[8] Ana Maria Mendonça and Aurélio Campilho, "Segmentation of retinal blood vessels by combining the detection of centerlines and morphological reconstruction," *IEEE Transactions on Medical Imaging*, vol. 25, no. 9, pp. 1200–1213, 2006.

[9] Muhammad Moazam Fraz et al., "An approach to localize the retinal blood vessels using bit planes and centerline detection," *Computer Methods and Programs in Biomedicine*, vol. 108, no. 2, pp. 600–616, 2012.

[10] Mariem Ben-Abdallah et al., "Automatic extraction of blood vessels in the retinal vascular tree using multiscale medialness," *International Journal of Biomedical Imaging*, vol. 2015, 2015.

[11] Mohammad Saleh Miri and Ali Mahloojifar, "Retinal image analysis using curvelet transform and multistructure elements morphology by reconstruction," *IEEE Transactions on Biomedical Engineering*, vol. 58, no. 5, pp. 1183–1192, 2011.

[12] Meindert Niemeijer et al., "Comparative study of retinal vessel segmentation methods on a new publicly available database," *Proc. SPIE 5370, Medical Imaging 2004: Image Processing*, pp. 648–656, 2004.

[13] Joes Staal et al., "Ridge based vessel segmentation in color images of the retina," *IEEE Transactions on Medical Imaging*, vol. 23, no. 4, pp. 501–509, 2004.

[14] João V. B. Soares et al., "Retinal vessel segmentation using the 2-D Gabor wavelet and supervised classification," *IEEE Transactions on Medical Imaging*, vol. 25, no. 9, pp. 1214–1222, 2006.

[15] Diego Marín et al., "A new supervised method for blood vessel segmentation in retinal images by using gray-level and moment invariants-based features," *IEEE Transactions on Medical Imaging*, vol. 30, no. 1, pp. 146–158, 2011.

[16] Ana Salazar-Gonzalez et al., "Segmentation of blood vessels and optic disc in retinal images," *IEEE Journal of Biomedical and Health Informatics*, vol. 18, no. 6, pp. 1874–1886, 2014.

[17] M. Elena Martinez-Perez et al., "Segmentation of blood vessels from red-free and fluorescein retinal images," *Medical Image Analysis*, vol. 11, no. 1, pp. 47–61, 2007.

[18] D. O. Dantas, "The VisionGL Library," http://github.com/ddantas/visiongl/.

[19] D. O. Dantas, H. D. P. Leal, and D. O. B. Sousa, "Fast 2D and 3D image processing with OpenCL," in *ICIP '15: IEEE International Conference on Image Processing Proceedings*. 2015, pp. 4858–4862, IEEE.

[20] E. R. Dougherty and R. A. Lotufo, *Hands-on Morphological Image Processing (SPIE Tutorial Texts in Optical Engineering Vol. TT59)*, SPIE Publications, July 2003.

[21] Augustina Bouchet et al., "Linguistic interpretation of mathematical morphology," in *Eureka-2013, Fourth International Workshop Proceedings*, 2013.

[22] Augustina Bouchet et al., "Arithmetic mean based compensatory fuzzy logic," *International Journal of Computational Intelligence and Applications*, vol. 10, no. 02, pp. 231–243, 2011.

[23] "STARE: STructured Analysis of the Retina," http://www.ces.clemson.edu/ahoover/stare/.

[24] "DRIVE: Digital Retinal Images for Vessel Extraction," http://www.isi.uu.nl/Research/Databases/DRIVE/.